Assessment of annual energy enhancement for tall building integrated with wind turbines (BIWT)

Farid Abdolhossein Pour[1], Matthew Herman[1], Robert Krawczyk[1]

[1]Illinois Institute of Technology, Chicago, IL

ABSTRACT: An emerging way to promote sustainability in the built environment is through the incorporation of wind power within buildings resulting in minimum transmission / distribution losses. Yet, the effectiveness of the proposed solutions are highly dependent on early integration of wind power systems with the architectural design process. Existing methods for aerodynamic evaluation of building forms are often not suitable for early design stage due to time and cost restrictions. As a result, the indicated methods often use over simplified conditions that omit the effect of local climate, surrounding terrain and building orientation. This paper, thus, intends to evaluate the effect of mentioned parameters on the annual energy output of a BIWT.

KEYWORDS: Building Integrate with Wind Turbine (BIWT), Wind Turbine, Onsite Energy Production

INTRODUCTION

This paper considers wind power as an important potential renewable energy source in tall buildings due to the possibility of accessing greater wind velocities at higher altitudes. In addition, air-flow patterns around buildings are considerably influenced by tall buildings' geometrical characteristics. Hypothetically, proper modification of building form can turn this unstructured phenomenon into a wind energy enhancement feature through the concentrator effect thus boosting the power production potential of tall buildings with an integrated wind turbine (BIWT). These aerodynamic modifications are typically evaluated via Computational Fluid Dynamic (CFD) or wind tunnel methods. These methods are often too expensive and time-consuming to analyze all annual fluctuations of local wind regimes (velocity, direction, and density) and thus can be inappropriate for use in early design stages when architectural concepts quickly evolve. Consequently, BIWT are often studied under simplified conditions (steady state analysis, single velocity, and angle) and under predicts the BIWT power coefficient and does not fully calculate the annual energy output. By disregarding the wide variety of other criteria influencing "annual energy output". These criteria include fluctuations of local wind regimes, adjacent terrain and building orientation (see Fig. 1).

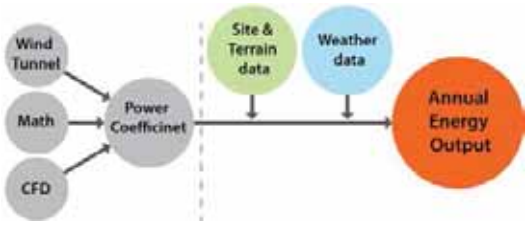

Figure 1: The Data Needed for Estimation of Annual Energy Output, from simplified Power Coefficient Calculations.

This paper intends to evaluate the suitability of BIWT power coefficient as a measure to inform the architectural integration of wind turbine into tall buildings design. The objective is to know whether a higher BIWT power coefficients always guarantee a greater annual energy output regardless of BIWT location and site. Thus, this paper intends to assess the sensitivity of "Local Weather", "Building Direction" and "Surrounding Terrain" on the BIWT annual energy output. The study outlines three BIWT case studies (sections 2.1, 2.2, and 2.3) and obtain the power coefficient profile using the provided math. Calculating the power coefficient profile for three BIWT case studies, the study carry on by approximation of Annual energy output for each case study at four different locations. The comparison of the annual energy productions tells how much local weather patterns, building direction, site terrain and the BIWT typology influence the annual energy output for a location.

1.0 HOURLY ANALYSIS

Based on the issues described in the introduction a research was proposed to streamline the study of BIWT, early in the architectural design process. To develop an appropriate methodology a detailed evaluation of precedent studies and methods were conducted. Many significant BIWT precedent researches reviewed in including the studies by Mertens (2006), Babsail (2011), and Campbell and Stankovic (2000). These evaluations leaded to a gap identification in BIWT filed of knowledge. The calculation procedures are presented below borrowed from precedent literature to describe a suitable methodology for predicting the

impact and potential benefits of BIWT for various tall building configurations. This work is part of ongoing research at the Illinois Institute of Technology, Collage of Architecture Ph.D. program.

1.1. Wind Turbine Power Calculation

According to mass conservation law, as long as density (ρ) and v are constant across an imaginary area of A, the total wind power content reads $P_{air} = ½\ \rho\ .v^3.\ A$ (Sathyajith, 2006; Stankovic, Campbell, and Harries, 2009). There is always some power losses associated with turbines. So, Per Equation [1], turbine power coefficient (C_p) is the fraction of extracted mechanical power out of total wind power content (Sathyajith, 2006).

$$P_t = ½\ C_p.\rho\ .v^3.A \qquad [1]$$

1.2. Terrain Roughness Length

The ground roughness depends on the local obstacles such as water, soil, trees, and urban areas (Sathyajith, 2006) and influences the wind velocity profile over the terrain. It described by the term "roughness length ($\boldsymbol{z_0}$)", which is provided for a set of selected surface types in Table 1 (Manwell, McGowan, and Rogers, 2002).

Table 1: Surface Roughness Length (approximate) by Terrain Type. Source: (Manwell et al., 2002)

Terrain Description	Roughness Length, $\boldsymbol{z_0}$ $(\boldsymbol{m})$
Snow surface	0.003
Fallow field / weather station standard surface type	**0.03**
Few trees	0.1
Forest and woodlands	0.5
Suburbs	1.5
Centre of cities with tall buildings	3.0

1.3. Historical Weather Data,

Historical weather data is often combined to create a typical meteorological representation of likely weather patterns. This process creates annual hourly data (8,760 hours) that represents long-term local climatic trends. Energy plus weather data (EPW) is one of the most accessible types of this data available for many locations in worldwide. EPW files are compliant with the most updated period of record from TMY2 and TMY3 datasets (Crawley et al., 1999). It contains wide variety of hourly data-fields including, wind speed (v), wind direction (α), atmospheric pressure (p) and dry bulb temperature (T). The data collection in weather stations takes place at a standard height (often 10 m) and terrain roughness of 0.03 m (Mertens, 2006). However, a BIWT is usually surrounded by an urban terrain different than standard terrain conditions where the weather data may be gathered. Also the turbine in BIWT is usually located at an elevation much taller than 10m. Thus, the data from EPW file cannot be directly employed for the calculation of energy production. In reality, in the absence of a practical technique for the measurements of the actual wind pattern at the required height, the alternative method is to extrapolate the wind velocity, angle and density from the surface data (EPW) to the BIWT situation. Sections 1.4, to 1.6 review the mathematical models used for the data extrapolation.

1.4. Hourly Wind Velocity at the Location of a Turbine

The following method is used by this study to provide adjusted wind velocity at the BIWT height from the surface data. To begin, the internal boundary layer (IBL) height and displacement height should be defined. The indicated parameters used later in the Log Law equation to calculate velocity at a given height (v_z).

IBL height: An abrupt change in the surface roughness (i.e. a city edge) creates a new boundary layer downwind of the step roughness (Fig. 2).It is called Internal Boundary Layer (IBL) and grows flowing forward. The effect of IBL is not present in the whole atmosphere but is limited to the height of IBL (h_k). Assuming the immediate roughness is $z_{0,1}$, faraway roughness $z_{0,2}$, maximum of $z_{0,1}$ and $z_{0,2}$ is $z_{0,\max}$ and distance from step roughness is x, Equation [2] estimate the IBL height (h_k) (ESDU82026, 2008; Mertens, 2006).

$$h_k(x) = 0.28.z_{0r}\left(\frac{x}{\max\left(z_{0,1}\,,z_{0,2}\right)}\right)^{0.8} \quad where\ \left[z_{0,\max} = Maximum\ of\ \ z_{0,1}\ \&\ z_{0,2}\right] \qquad [2]$$

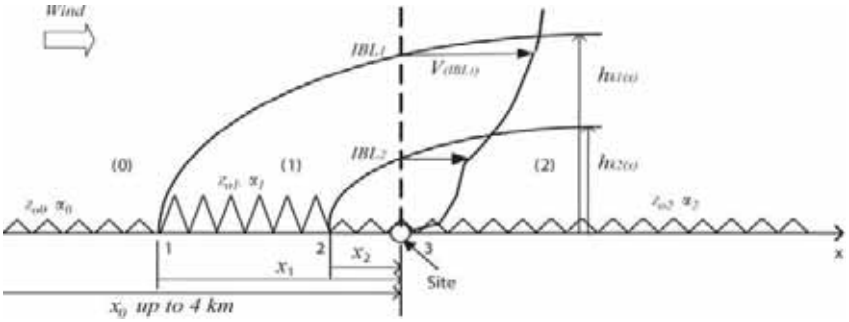

Figure 2: Internal Boundary Layers (IBL) above a Fetch, adopted from (Wang and Stathopoulos, 2007)

Displacement Height: Measurements of the velocity profile over a very rough terrain such as urban regions indicates a vertical displacement of the entire flow regime for those surfaces (Emeis, 2012). The displacement height (d) for the surfaces with low roughness is negligible, and would be disregarded. However, for the case of a typical city, d is approximately estimated around 23m (ESDU82026, 2008; Mertens, 2006)

Log law: To extrapolate the surface wind speed data to an alternative site (with diverse terrain condition and height), Sathyajith (2006) makes a logical assumption that velocity is not noticeably influenced by the terrain characteristics above a certain height. Thus, the velocity for a new location can be found by matching the velocities of the reference site and the new location at that height. For low roughness, this height is taken 60m above the ground (Lysen, 1983). Thus, the log law results in Equation [3] when v_{z_R} and z_{0R} are velocity and roughness lengths at reference site (e.g. EPW data) and $v_{(Z)}$ and z_0 are velocity and roughness length at the new location respectively, (Mertens, 2006; Sathyajith, 2006). Per section 1.3, the EPW standard condition is $z_R = 10m$ and $z_{oR} = 0.03m$, so the original log law yields it new form in Equation [3] (Mertens, 2006).

$$v_z = \frac{Ln\left({}^{60}/_{z_{0R}}\right)\ Ln\left({}^{Z}/_{z_0}\right)}{Ln\left({}^{60}/_{z_0}\right)\ Ln\left({}^{Z_R}/_{z_{0R}}\right)}\ v_{z_R} \quad \xrightarrow{yields} \quad v_z = 1.31\ \frac{Ln\left({}^{Z}/_{z_0}\right)}{Ln\left({}^{60}/_{z_0}\right)}\ v_{z_R} \qquad [3]$$

Log law for High roughness: For a city or a very rough terrain, the wind may experience multiple step roughness from the standard terrain of the weather station (z_{oR}) to the roughness of surrounding suburban regions (z_{01}) and the roughness of the city itself (z_{02}) see Figure 2. By matching the velocity above and below IBL height $h_k(x)$, the velocity profile in IBL_2 can be calculated by surface reference velocity from EPW file, therefore the Equation [3] evolves to Equation [4] (Mertens, 2006; Sathyajith, 2006).

$$v_z = 1.31\ \frac{Ln\left({}^{h_k}/_{z_{o1}}\right) Ln\left({}^{[z-d]}/_{z_{o2}}\right)}{Ln\left({}^{60}/_{z_{01}}\right) Ln\left({}^{[h_k-d]}/_{z_{o2}}\right)}\ v_{z_R} \qquad [4]$$

1.5. Hourly Air Density at the Location of a Turbine

Per Equation [1], air density (ρ) is directly proportional with Turbine output energy. The surface air density (ρ_0) can be estimated using Ideal gas Law as illustrated in Equation [5], (U.S. Standard Atmosphere, 1976).

$$\rho_0 = {}^{RT}/_{p}\ [\text{where } T \text{ is } °K = (°C\ +\ 273.15)] \qquad [5]$$

Where T is absolute dry bulb temperatures in $°K$ (note that temperature in EPW file is provided in $°C$), R is universal gas constant for air ($R = 8.31432\ J/mol.°K$) and p is atmospheric pressure obtained directly from EPW weather data. However, both p and T change as function of attitude. The U.S. Standard Atmosphere 1976 provides another equation based on Ideal gas Law and changes of p and T that is called Barometric formula as shown in Equation [6], where $\Gamma e = $~6.5°C/km is environmental lapse rate of temperature, and $g = 9.80665\ \text{m/s}^2$ is gravitational acceleration (U.S. Standard Atmosphere, 1976).

$$\rho = \rho_0 \left(\frac{T_0}{T_0 + \Gamma e.(H - H_0)}\right)^{\left[\frac{g}{R.\Gamma e}\right]+1} \qquad [6]$$

2.0 BUILDING INTEGREATED WITH WIND TURBINE (BIWT)

BIWT refers to wind turbines that operate in a wind concentrated by a building. The integration method of turbines and buildings includes top, side and duct installation and installation between multiple towers

(Stankovic et al., 2009, P22). Mertens (2006) has done an aerodynamic investigation on wind energy production in the built environment. The study provides remarkable mathematical methods for quick estimation of BIWT power coefficients for three BIWT typologies including turbines at the buildings' roof, airfoil concentrators and bluff concentrators. These Mathematical formulas are partially validated using CFD analysis and wind tunnel testing. This paper focuses only on airfoil and bluff concentrators from his study.

2.1. Bluff Concentrator

The mathematics presented here, are borrowed from Mertens (2006 pp. 124-138) to explores the performance of a turbine placed between twin bluff shape buildings. Bluff bodies are characterized by early and quick flow separation from the body surfaces. An adverse pressure gradient between upwind and downwind surfaces induces flow velocity in connections or ducts between high and low pressure areas (Figure 3 and 4).

Jet contraction: When flow is crossing a sharp edge nozzle, the jet diameter is often less than the nozzle diameter. This is the result of the fluid inability to turn the sharp corners. The ratio between the smallest flow area and the nuzzle area is called jet contraction coefficient $(\beta = A_t/A_f)$ as shown in figure 3. Also, the flow around the axi-symmetric plate concentrator is displayed in Figure 4.

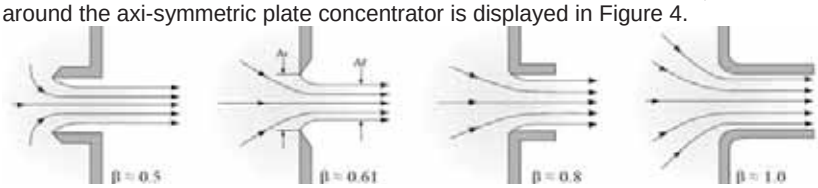

Figure 3: Jet Contraction (β) for Different Edge Configuration. Adopted from (Munson et al, 2009)

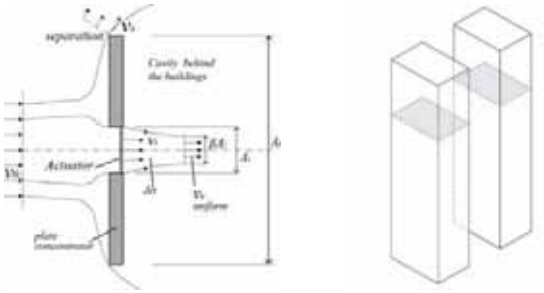

Figure 4: The Plate Concentrator in Axial Parallel Flow (Plan view). Adopted (Mertens, 2006)

According to Mertens (2006), power coefficient of a bluff concentrator ($C_{P,Bluff}$) is obtain from Equation [7].

$$C_{p,bluff} = \frac{2\,\beta}{3\sqrt{3}} \left(\frac{v_s}{v_0}\right)^3 \qquad [7]$$

Where v_s separation velocity (see Fig. 4), v_0 is ambient wind velocity and β is Jet contraction (see Fig 3). As wind approaches a building, the surrounding flow patterns are noticeably dependent on the dimensional ratio of the building / BIWT form. The bodies with similar lengths in three dimensions deflect flow in all three dimensions (3D bodies). But, for the bodies with one length noticeably larger than other dimensions, as found with tall buildings, tend to deflect the flow on a 2D plane over the building's smaller section (Abdolhossein Pour, 2014; Hoerner and Borst, 1975). Mertens (2006) indicates that for 2D bluff bodies $v_s/v_0 \approx 1.3$ while for 3D bluff bodies $v_s/v_0 \approx 1.2$. Accordingly, Equation [7] for a tall BIWT (2D body) with rounded edges ($\beta = 1$) gives $C_{p,bluff} = 0.85$. Mertens measurements, reports a 30% reduction in $C_{p,bluff}$ for yawed flow of $\varphi = 45°$. The profile of Bluff concentrator power coefficient is shown in Table 2 when $C_{p,0°}$ and $C_{p,180°}$ are power coefficients at $\varphi = 0°$ and $\varphi = 180°$.

Table 2: Normalized Power Coefficient as Function of Yaw Angle. Source (Mertens, 2006)

yaw angle (φ)	0°	45°	90°	135°	180°
Normalized $C_{p,bluff}$	$C_{p,0°}$	70% $C_{p,0°}$	0	70% $C_{p,180°}$	$C_{p,180°}$

2.2. Arifoil Concentrator (Shrouded Turbines)

The following section and equations, are borrowed from Mertens (2006 pp. 97-123) and investigates the performance of a BIWT with twin symmetrical airfoil shape concentrators (see Fig. 5). Mertens reports that a

shrouded turbine power coefficient ($C_{P,shroud}$) for a perpendicular flow is calculated from Equation [8], Where C_l is the Airfoils lift coefficient, c is the airfoils chord length, D_t is turbine diameter and X_s and X_a are correction factors and are obtained from Equations [9] and [10].

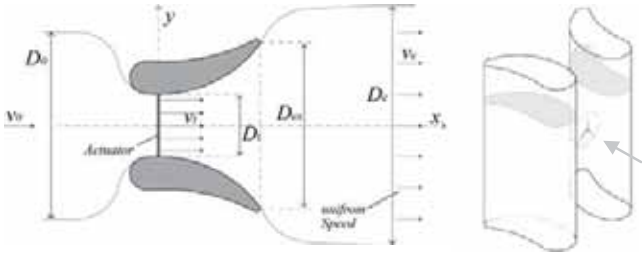

Figure 5: A Shrouded Configuration. Adopted from (Mertens, 2006)

$$C_{P,shroud} = \frac{16}{27}\left(\frac{X_a C_l c}{\pi D_t}\,\frac{1}{1-\dfrac{X_s C_l c}{4\pi D_t\left(1+\left(\dfrac{c}{2D_t}\right)^2\right)}}\right) \qquad [8]$$

$$X_a = 0.5051\, ln\left(\frac{D_t}{2c}\right) + 1.4447 \quad if \quad 0.2 \le \frac{D_t}{2c} < 5 \qquad [9]$$

$$X_s = \frac{1}{1-0.0511\left(\dfrac{D_t}{2c}\right)^{-1.6211}} \quad if \quad \frac{D_t}{2c} \ge 0.3 \qquad [10]$$

However, $C_{P,shroud}$ from Equation [8] is valid only for perpendicular flows toward the building. In the case of yawed flow, $C_{P,shroud,\varphi}$ decreases as a function of the yaw angle (φ). Mertens reports, from Phillips, Flay, and Nash (1999), the measurements of $C_{P,shroud,\varphi}$ for yawed flow. The measurements indicated that the power coefficient is changing by φ but remain proportional to $C_{P,shroud,0^\circ}$ (perpendicular flow). Table 3 illustrates the ratio of power coefficient at different yaw angles normalized to $C_{P,shroud,0^\circ}$.

Table 3: Normalized Power Coefficient as Function of Yaw Angle. Source (Phillips et al., 1999)

yaw angle (φ)	0°	5°	10°	15°	20°	30°	40°	45°
Normalized $C_{P,shroud,\varphi}$	100%	100.4%	99.1%	91.5%	86.0%	80.8%	68.0%	62.5%

For range of $\varphi = 90°$ to $180°$, the sharp edge of airfoils results in early flow separation, so the flow across the airfoils effectively behaves like across bluff bodies (see section 2.1, bluff bodies). Accordingly the power coefficient for $\varphi = 90°$ to $180°$ is calculated using Equation [7] and Table 2. As result $C_{P,shroud,90^\circ} = 0.77$ and $C_{P,shroud,180^\circ} = 0.85$, are not dependent of $C_{P,shroud,0^\circ}$, the airfoil shape and angle of attack and remain almost constant for different airfoil geometries.

2.3. Combined Concentrators

Airfoil and bluff BIWTs show relatively high sensitivity to yaw angle. This sensitivity greatly drops their annual output power for omnidirectional winds. Mertens (2006) proposes two identical bluff concentrators in cross configuration (See Fig. 6) to solve this problem. The idea is denoted as the *combined concentrator* in this paper. This configuration is proposed in an attempt to significantly increase C_p for $\varphi = 90° \,\&\, 270°$ (see Figure 6). Since sharp edges buildings are expected to be inefficient, Mertens focuses only on airfoil shapes buildings for combined concentrators. The combined concentrator power coefficients are shown in Table 4.

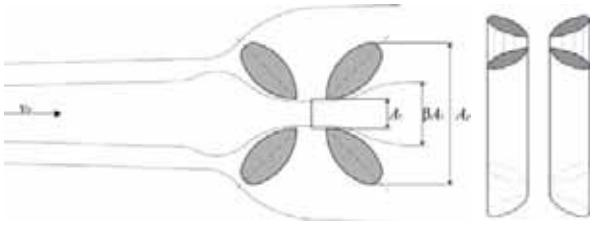

Figure 6: Combined Plate Concentrator at $\varphi = 45°$. Adopted from (Mertens, 2006)

Table 4: Power Coefficient as Function of Yaw Angle. Source (Mertens, 2006)

yaw angle (φ)	0°	45°	90°	135°	180°
$C_{P,combined}$	0.51	1.01	0.51	1.01	0.51

3.0 CASE STUDIES

Three case studies are presented below in sections 2.1 to 2.3 and summarized in figure 7. Also, the turbine diameter, the tower's height, the turbine height, as well as the number of the floors are assumed to be constant and equal to 30m (98.5ft) and 250m (820ft), 200m (656ft) and 65m respectively for all cases. Hence, variations in the results are purely due to the BIWT power coefficient and the weather data and BIWT direction.

- ***Airfoil Concentrator****:* For this case study the selected shape is GOE435-il with C_L =1.7543 at attack angle (α) of 17.5° and c = 50m (164ft) (Airfoil Tools, 2013)[1].
- ***Bluff Concentrator****:* This case study uses twin towers with dimension 60m by 35m (197ft by 115ft) for each tower, figure 7, middle. The floor depth of 35m (115ft) gives a lease span of about 13m (40ft) as well as 40ft for a central core. The front and back inlet edges are chosen to be well rounded (β1=β2=1).

- ***Combined Concentrator****:* This case study is composed of four towers in a cross configuration. Each tower is a symmetrical airfoil with a chord length of 60m (197ft) and thickness of 27.5m (90ft).

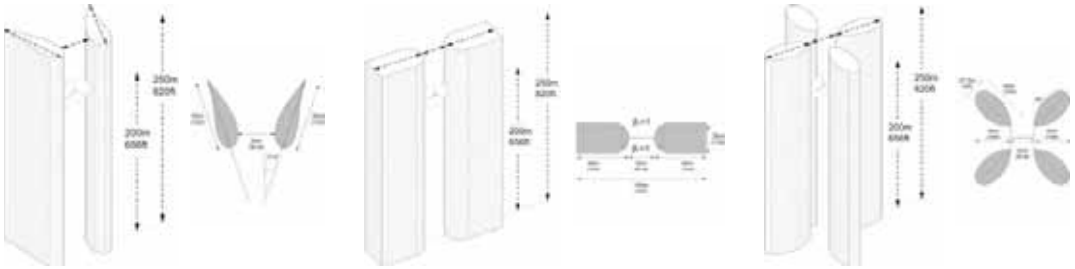

Airfoil Concentrator | Bluff Concentrator | Combined Concentrator

Figure 7: Three BIWT case studies, corresponding to the three BIWT typologies in sections 2.1, 2.2, and 2.3

The profile of power coefficients for each case study has been calculated using the data and mathematical equations provide in sections 2.1 to 2.3. This part of the analysis is donated as "Steady state analysis". The power coefficient profile for three case studies are illustrated in Figure 8. For perpendicular flow, $C_{P,shroud,0°}$ (Fig. 8, right) is highest among the case studies. However, both airfoil and bluff concentrators (figure 8, right and middle) show a relatively high sensitivity to the wind angle. The combined concentrator shows lower power coefficients in all directions comparing $C_{P,shroud,0°}$ but characterizes minimum sensitivity to the yaw angle. The best BIWT case study, is the one capable of maximizing energy production. Nonetheless, with only a steady state power coefficient, it is still not possible to predict which option will produce more energy.

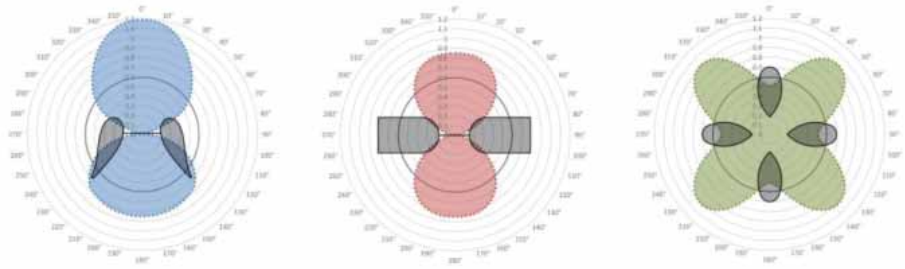

Figure 8: Three BIWT case studies, corresponding to the three BIWT typologies in sections 2.1, 2.2, and 2.3

The next step of the study is applying annual hourly weather data in the calculation of annual energy production, denoted as "hourly dynamic analysis". Incorporation of steady state (Figure 8) and hourly dynamic analyses results in the calculation of annual energy production. To test the usefulness of this methodology four cities were selected for study based on wind speed and the wind angle distribution profile. The cities are intentionally chosen with diverse wind patterns, latitudes and climates so, the influence of weather data on annual energy enhancement of each BIWT typology is exemplified. The selected cities are Chicago, New York, Berlin and Abu Dhabi. Their wind patterns are shown in Figure 9.

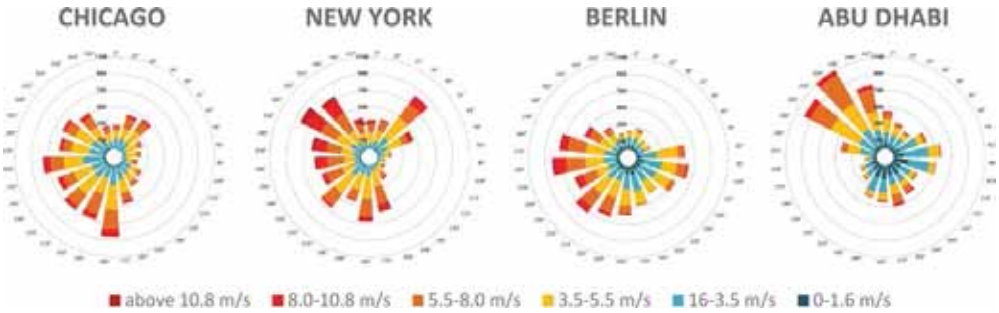

Figure 9: Wind Rose at the Ground and the Turbine Height

3.2. BIWT Orientation (Azimuth)

Assuming hourly wind angle and BIWT orientation measured clockwise from North are respectively α_w and θ, the wind yaw angle of BIWT (φ) is obtained from $\varphi = \alpha_w - \theta$. So φ depends on both θ and α_w. So, It is also important to study the effect of BIWT alignment (θ) on the total annual energy enhancement. In this study, the annual energy production of BIWT is obtained for 36 direction in 360°, while θ was changing in 10° increments.

3.3. Algorithmic Procedure of the Study

The study was further developed through the application of hourly annual weather data (EPW file) for the calculation of annual energy production of the three indicated case studies in each city for each angular increment of θ. The hourly power production of a BIWT is obtained from substitution of the Equations [4] and [6] and as well as results from tables 2, 3 and 4 into Equation [1]. The hourly energy production of a BIWT, thus, is obtained from Equation [11] where, T is the period of time and equal to 1 hour for hourly data (EPW).

$$E_T = ½\, C_{P_\varphi}.\ \rho_z\ .{v_z}^3.A_t.T \qquad [11]$$

The following steps have been done for each case study in each city.

Step 1. BIWT direction is assumed toward north for all case studies (θ =0°)
Step 2. Extrapolation of wind velocity for the BIWT height using Equations [3] or [4] from the surface data
Step 3. Calculation of air density for the BIWT height using Equation [6]
Step 4. Calculation of power coefficient profile for three BIWT case studies as shown in Figure 9.
Step 5. Substituting the results from last 3 steps in Equation [11] to obtain hourly energy (E_t)
Step 6. Summation of Hourly result over a year is annual energy output of the BIWT ($E_{BIWT} = \sum_{T=1}^{8760} E_T$)
Step 7. E_{BIWT} is obtained assuming BIWT direction is θ at step 1
Step 8. Modifying the BIWT direction incrementally with 10° increment, and redo the steps 2 to 7

The last step of the proposed methodology uses an algorithmic process to produce an optimization loop of with array of 36 analysis scenarios for each BIWT/City while θ is incrementally changing. At step 8, θ increase by 10° and the whole calculation process is repeated for new value of θ. Analysing 3 case studies in four cities at 36 angles give the total of 432 annual energy production measurements for this study. Each array of 36 studies creates the annual energy production profile of a BIWT/City as a function θ shown as a radar or circular charts for three case studies and 4 cities in Figure 10. Each colour corresponds to one BIWT typology.

Figure 10: Energy production profile as functions BIWT alignment, the most efficient BIWT in each city is shown in a dash line rectangles. Also the best orientation of BIWT is shown with white arrows.

3.4. Analysis of the Results

Surprisingly, the peak production came from the “Combined Concentrator” located in New York. Similarly, Chicago’s best BIWT typology was the “Combined Concentrator” too (Fig. 10). Berlin and Abu Dhabi benefited most from the “Airfoil Concentrator” configuration. In all cities, the “Bluff Concentrators” produced less than other BIWT typologies. In general, a concept with an excellent performance in one city might not

be appropriate for another city depending on the local pattern of wind velocity and angle. For instance, cities like Chicago that do not have a dominant wind direction, the omni-directional concept (Combined Concentrator) works better though it shows lower power coefficient. For a place with dominant wind direction, like Abu Dhabi, the Airfoil concentrator shows the best performance out of the three configurations studied.

3.5. Conclusion

This paper demonstrates the application of a methodology which accounts for local wind and terrain conditions that impact the annual power output of a BIWT. The case studies presented, indicate, it is possible that a BIWT with lower power coefficient produce more annual energy depending on specific terrain conditions, local annual wind pattern, power coefficient of BIWT and its sensitivity to the yaw angle. It can be concluded that power coefficient is not the only parameter influencing the ultimate BIWT energy production. Thus, the use of power coefficient to inform the architectural design process of BIWT, while disregarding other important parameters (e.g. local weather data, terrain condition) might be misleading for the design team. The “Algorithmic Procedure” described briefly in section 3.3, is part of an ongoing research and tool development for an accurate and quick estimation of BIWTs’ annual energy improvement in early design stages. The final decision on the use of BIWT should be made by the design team based on all associated design criteria and cannot be prescribed before the design process starts. Thus, the proposed tool for identifying the best BIWT typology and its optimum angle can possibly be an important part of a BIWT design process. As a result, the design team take the right direction when there is still time for extensive modifications in building architecture.

ACKNOWLEDGEMENTS

Sincere gratefulness to Dr. Dietmar Rempfer, Professor of aerospace engineering, and Dr. Hamid Arastoopur, Professor of chemical engineering at Illinois Institute of Technology, for their supports during this research.

REFERENCES

Abdolhossein Pour, F. (2014). *Evaluation of Tall Office Building Form to Enhance Wind Energy Production in Building Integrated Wind Turbine, a Performance Based Approach for Early Design Stage*. (Ph.D. Dissertation), Illinois Institute of Technology, Chicago.

Airfoil Tools. (2013). *Airfoil Tools*. Retrieved October 1, 2013, from http://airfoiltools.com

Babsail, M. O. (2011). *Toward Net Zero Energy: The Correlation between Architectural Forms of Tall Buildings and Wind Power Production*. (Ph.D. Dissertation), Illinois Institute of Technology.

Campbell, N. S., and Stankovic, S. (2000). *Wind Energy for the Built Environment. (Project WEB). Assessment of Wind Energy Utilisation Potential in Moderately Windy Built-up Areas*. London BDSP Partnership.

Crawley, D. B., Lawrie, L. K., Winkelmann, F. C., W.F. Buhlc, Y. J. H., Pedersen, C. O., Strand, R. K., . . . Glazer, J. (1999). *EnergyPlus, A New-Generation Building Energy Simulation Program*. Paper presented at the Building Simulation '99, Kyoto, Japan.

Emeis, S. (2012). *Wind Energy Meteorology: Atmospheric Physics for Wind Power Generation*: Springer.

ESDU82026. (2008). *Engineering Sciences Data Unit: ESDU International plc*.

Hoerner, S. F., and Borst, H. V. (1975). *Fluid-dynamic lift: practical information on aerodynamic and hydrodynamic lift*; [information on lift and its derivatives, in air and in water]: Hoerner Fluid Dynamics.

Lysen, E. H. (1983). *Introduction to Wind Energy: Basic and Advanced Introduction to Wind Energy with Emphasis on Water Pumping Windmills*: Consultancy Services Wind Energy Developing Countries.

Manwell, J. F., McGowan, J. G., and Rogers, A. L. (2002). *Wind Energy Explained: Theory, Design and Application*: West Sussex, UK, Wiley.

Mertens, S. (2006). *Wind Energy in the Built Environment: Concentrator Effects of Buildings*. (Ph.D Dissertation), Technische Universiteit Delft, Brentwood, Essex.

Munson, B. R., Young, D.F., Okiishi, T.H., Huebsch, W.W. (2009). *Fundamentals of fluid mechanics*: Wiley.

Phillips, D. G., Flay, R. G. J., and Nash, T. A. (1999). *Aerodynamic Analysis and Monitoring of the Vortec 7 Diffuser-Augmented Wind Turbine*. IPENZ Transactions, 26(1), 13-19.

Sathyajith, M. (2006). *Wind Energy: Fundamentals, Resource Analysis and Economics*: Springer.

Stankovic, S., Campbell, N., and Harries, A. (2009). *Urban Wind Energy*: Earthscan.

U.S. Standard Atmosphere. (1976). National Oceanic and Atmospheric Administration, National Aeronautics and Space Administration, US Air Force

Wang, K., and Stathopoulos, T. (2007). E*xposure model for wind loading of buildings*. Paper presented at the The Fourth European and African Conference on Wind Engineering, Journal of Wind Engineering and Industrial Aerodynamics.

ENDNOTES

[1] The website’s offer a database of 1629 airfoils, searchable by name, thickness and camber. The lift coefficient data as a function of attack angle is available for most airfoil within the database.